Int. J. Heat Mass Transfer. Vol. 16, pp. 755–768. Pergamon Press 1973. Printed in Great Britain

BUOYANT PLUME ABOVE A HORIZONTAL LINE HEAT SOURCE

TETSU FUJII, ITSUKI MORIOKA and HARUO UEHARA
Research Institute of Industrial Science, Kyushu University, Fukuoka, Japan

(*Received* 1 *December* 1971)

Abstract—The first problem dealt with in this paper is the solution of the equations concerning the steady laminar plume above a horizontal line heat source. While there are some controversies raised against what is proposed on this problem by Gebhart *et al.* [1], new numerical solutions which are more accurate are presented for $Pr = 0{\cdot}01$, $0{\cdot}03$, $0{\cdot}1$, $0{\cdot}3$, $0{\cdot}7$, 1, 3, 5, 10, 30 and 100. Furthermore, the profiles of vertical velocity component and temperature are graphed so that there may be convenience of interpolation for an arbitrary Prandtl number.

The relation between theory and experiment is taken up for consideration, by reviewing all-inclusively the results of experiments made on the plumes in air, water and spindle oil as well as those hitherto reported on air and liquid silicone. While the natural motion of plume left undisturbed is extremely slow, it is considerably resembled to the fluttering of a flag. The photographs offered here represent typical motion of the plume in spindle oil. Generally speaking, experimental results are different from theories, but, so far as the temperature distribution in the plume is concerned, the similarity variable corresponding to the theory is applicable to it. The maximum temperatures in the plumes in air were about 15–20 per cent lower than the theoretical predictions in the whole range of Grashof number. Those in water and spindle oil were in good agreement with the theoretical predictions in the range of about $Gr < 10^6$.

NOMENCLATURE

f, dimensionless stream function;
$f(\infty)$, dimensionless vertical flow rate;
f', dimensionless vertical velocity component;
$f'(0)$, eigenvalue of f';
F, dimensionless stream function used by Gebhart *et al.*;
g, gravitational acceleration;
Gr, Grashof number defined by (8);
h, dimensionless temperature;
$h(0)$, eigenvalue of h;
H, dimensionless temperature used by Gebhart *et al.*;
I, normalyzing constant given by (10);
J, constant defined by (21);
Pr, Prandtl number;
Q, heat rate per unit length of the line heat source;
t, fluid temperature above the ambient temperature;
t_0, temperature on the mid-plane of plume or maximum of t measured at x;
u, vertical velocity component;
x, elevation above the line heat source;
y, horizontal distance from the mid-plane of plume.

Greek symbols

β, volumetric thermal expansion coefficient;
δ, temperature layer thickness defined in (12);
η, dimensionless coordinate used by Gebhart *et al.*;
Θ, number with dimension of temperature defined by (9);
λ, thermal conductivity;
ν, kinematic viscosity;
ξ, dimensionless coordinate defined by (7);

1. INTRODUCTION

WHEN a horizontal line heat source is placed in a quiescent fluid, there is formed a layer. This is called buoyant plume or natural convection plume.

Concerning the theoretical treatment of the steady laminar plume, Gebhart *et al.* [1] have written an inclusive paper, which has, however, some doubtful points. In the first place, though the literature survey is significant and useful, a mistake of closed form solutions is quoted without correcting it. In the second place, the discussion of apparent redundancies in boundary conditions, which pertains to one of the fundamental characteristics of pertinent differential equations, is mathematically questionable. In the third place, the reliability of numerical solutions proposed for $Pr = 0{\cdot}1$, $0{\cdot}7$, $6{\cdot}7$ and 10 falls short of the indicated significant figures. Furthermore, the results for $Pr = 0{\cdot}01$ and 100 are useless, since real values of velocity and temperature field cannot be obtained according to what they proposed in their paper.

Recently, Soward [2] analyzed buoyant convection in a vertical magnetic field. Brodowicz [3] applied the theoretical results of thermal buoyant convection to the treatment of the experimental data of diffuse buoyant convection. Savage–Chan [4] treated a buoyant two-dimensional laminar vertical jet, taking account of the initial conditions of the momentum flux. Under these circumstances it is considered preferable to represent accurate numerical solutions for a wide range of Pr number, since the numerical calculation is very tedious and is liable to cause errors.

The first object of the present paper is to propose more accurate numerical solutions after commenting on the work of Gebhart *et al.*

Concerning experimental studies the authors have three recent papers of [5–7] ready in hand. Brodowicz–Kierkus [5] grasped the whole characteristics of the plume in air by measuring the temperature and velocity distribution, using a Mach–Zehnder interferometer and dust-particle trajectory respectively. Main points obtained are listed as follows; (i) The vertical velocity component is generally higher, the temperature on and near the vertical plane, including the heat source, is lower and the width of the plume is more expanded, in comparison with those of the theoretical prediction. (ii) Because of the boundary layer of about one centimeter diameter formed around the heat source, a velocity field is brought forth under the heat source, too. The entrance velocity from the ambient to the plume is slightly inclined downwards instead of being strictly horizontal. These facts are discrepant with the theoretical assumption. (iii) Both distributions of temperature and velocity are not strictly symmetrical with respect to the vertical plane including the heat source.

Forstrom–Sparrow [6] contrived an enclosure, which isolated the plume in air from the surroundings. The temperature profile in the plume was measured by a thin thermocouple over wide ranges of heat rates and elevations above the heat source. A traversing apparatus assembled in the enclosure was remotely controlled. It may be appreciated that they discovered the following new facts through their study. (iv) The laminar plume displays a slow, regular swaying motion, which is regarded as one of the characteristics of buoyant plumes. (v) The onset of transition to turbulence occurs at $Gr = 5 \times 10^8$, and fully turbulent conditions prevail at $Gr = 5 \times 10^9$.

Schorr–Gebhart [7] measured the temperature profile in the plume in liquid silicone of $Pr = 6{\cdot}7$ by means of a Mach–Zehnder interferometer. They established an ideal test condition by minimizing the minor circulation caused by both the walls of the test tank and the plume itself, and by reducing the variation of the physical properties with temperature. A slight twist observed in the fringes in the photo, however, seems to show that the swaying motion is not arrested completely. All facts discovered may be as follows; (vi) The necking in of the plume takes place owing to the non-infinite length of the heat source.

Forstrom–Sparrow and Schorr–Gebhart both asserted that they could make the temperature profile agree excellently with theory by accurate measurements. It is, however, unlikely that the temperature profile in the plume, which accompanies the swaying motion, is in agreement with the theoretical prediction concerning steady condition.

Pera–Gebhart [8] performed theoretical calculation on the stability of plume and its experimental varification with using air. The unstable flow treated in their paper, however, seems to be different from above-mentioned swaying motion.

The authors experimented on the plumes in air, water and spindle oil, but they adopted no special measures to stabilize them in each case.

The second aim of the present paper is to discuss on the relation between the theory and phenomena, based on the several results mentioned above.

2. CONSIDERATION ON THE THEORETICAL TREATMENT

The problem is concerned with solving the following differential equations

$$f''' + \tfrac{3}{5}ff'' - \tfrac{1}{5}f'^2 + h = 0, \tag{1}$$

$$h'' + \tfrac{3}{5}Pr(hf)' = 0, \tag{2}$$

subject to the boundary conditions

$$f'' = f = h' = 0 \quad \text{at} \quad \xi = 0, \tag{3}$$

$$f' = h = 0 \quad \text{at} \quad \xi \to \infty, \tag{4}$$

where the prime denotes differentiation with respect to ξ.

The vertical velocity component u and temperature t are expressed as

$$u = \nu Gr^{\frac{1}{2}} f'/x, \tag{5}$$

$$t = Gr^{-\frac{1}{4}}\Theta h, \tag{6}$$

where

$$\xi = Gr^{\frac{1}{4}} y/x, \qquad Gr = x^3 g\beta\Theta/\nu^2, \tag{7),(8}$$

$$\Theta = Q/I\lambda Pr, \qquad I = \int_{-\infty}^{\infty} f'h\,\mathrm{d}\xi. \tag{9),(10}$$

The conservation of momentum is expressed as

$$\int_{-\infty}^{\infty} f'^2\,\mathrm{d}\xi = \tfrac{5}{4}\int_{-\infty}^{\infty} h\,\mathrm{d}\xi. \tag{11}$$

The temperature layer thickness δ is defined by the following formula,

$$2\int_{-\delta/2}^{\delta/2} h\,\mathrm{d}\xi = \int_{-\infty}^{\infty} h\,\mathrm{d}\xi. \tag{12}$$

For details of the above equations and definitions refer to [9].

2.1 *Closed form solutions*

Yih [10] presented closed form solutions for $Pr = \frac{2}{3}$ and $\frac{7}{3}$. It is assumed intuitively in his analysis that dimensionless profiles of vertical velocity component and temperature are expressed by a power of hyperbolic function. The solutions obtained by the above assumption, however, are confined to the cases of $Pr = \frac{5}{9}$ and 2, which correspond to the cases deduced by Crane [11] and Fujii [9] respectively. Yih's mistake comes from his arithmetic operations.

Solutions normalized by (17) for $Pr = \frac{5}{9}$ are as follows;

$$f' = \left(\frac{675}{2048}\right)^{\frac{1}{4}} \operatorname{sech}^2\left(\frac{5}{768}\right)^{\frac{1}{4}}\xi, \tag{13}$$

$$h = \left(\frac{3}{640}\right)^{\frac{1}{4}} \operatorname{sech}^2\left(\frac{5}{768}\right)^{\frac{1}{4}}\xi. \tag{14}$$

2.2 *Boundary conditions*

Equation (2) is solved subject to the second and third conditions of (3) as

$$h = h(0)\exp\left(-\tfrac{3}{5}Pr\int_0^{\xi} f\,\mathrm{d}\xi\right), \tag{15}$$

where $h(0)$ is an eigenvalue of h. Since f is positive and becomes constant for large ξ, $\lim_{\xi\to\infty} h = 0$. Therefore, the last condition of (4) given by a physical consideration is not independent. The brief summary given above is the beginning of the discussion of Gebhart *et al.* [1] on the redundancies in boundary conditions.

Since the above-mentioned relation

$$\lim_{\xi \to \infty} f = \text{positive constant} \tag{16}$$

is one of the characteristics of the solutions of (1) and (2), it is unreasonable to give this condition before solving them. It is still reasonable that the boundary conditions generated definitely from physical condition are confined to five of (3) and (4).

While n boundary conditions are generally indispensable and sufficient to solve the nth order system of differential equations, the uniqueness of the solution is never assured. The fact that (1) and (2) have an infinite number of solutions is one of the characteristics of these equations. Fujii [9], therefore, introduced a normalizing condition as

$$\int_{-\infty}^{\infty} f'h \, d\xi = 1. \tag{17}$$

It may be considered that the condition

$$h(0) = 1 \tag{18}$$

employed by Gebhart *et al.* is the substitution for (17). If necessary, it may be substituted by

$$f'(0) = 1 \tag{19}$$

or by other conditions as shown in [4, 12], because the present problem is one eigenvalue problem as plain from I.3 of [9]. For the calculation of real values of velocity and temperature, however, none of these conditions of (17)–(19) etc. is necessary, if only the value of integral (10) is available. On the contrary, the real values cannot be obtained without this integral value. In solving (1) and (2) it is convenient to assume the value of $h(0)$ properly and find out the corresponding $f'(0)$, because h approaches monotonously to zero because of the characteristics of (2) or (15).

Gebhart *et al.* misunderstood the statement "the theoretical or numerical calculation cannot be performed without this condition" in the footnote of Fujii's paper [9]. This statement concerns the solution of Spalding–Cruddace [13], and this condition in the quotation denotes that $f = 0$ at $\xi = 0$.

In short, the method of Gebhart *et al.* is equivalent to Fujii's instead of being so "clear, very simple and efficient". It is to be noted here that the transformation proposed by Gebhart *et al.* has been already derived by Katto–Koide [14] in more general way.

3. NUMERICAL RESULTS

Numerical calculations are performed for $Pr = 0{\cdot}01$, $0{\cdot}03$, $0{\cdot}1$, $0{\cdot}3$, $\frac{5}{9}$, $0{\cdot}7$, 1, 2, 3, 5, 10, 30 and 100 by using Runge–Kutta method. Eigenvalue $f'(0)$ is searched out for a fixed value of $h(0)$, based on the results of Uehara–Fujii [15] and Fujii [9]. Thereafter f' and h are normalized by using relation (17). When an estimated value of $f'(0)$ is slightly smaller than a presumable exact value, f' decreases monotonously and takes a negative sign over the range of a large value of ξ. On the other hand, when the value $f'(0)$ is slightly larger, f' becomes to increase at a point of ξ, where f' takes a small positive value shown in the last column of Table 1. The values of f and h up to this point, which is an inflextion point of f, are employed as representative solutions, since the condition at $\xi \to \infty$ cannot exactly be satisfied in the digital computation.

The obtained dimensionless profiles of vertical velocity component and temperature are shown in Figs. 1 and 2. The characteristic values of solution, accuracy and calculation are summarized with respective significant figures in Table 1.

When compared with closed form solutions for $Pr = \frac{5}{9}$ and 2, the numerical results are assessed to be accurate to respective significant figures. The accuracy for conservations of momentum and energy is achieved to the order of 10^{-5} in the range of $Pr \geqslant 0{\cdot}1$. The results obtained for $Pr = 0{\cdot}01$ and $0{\cdot}03$ were not so accurate as those for the other Pr number, because they are still deficient in the significant figures of the eigenvalues.

Comparison between the results of Gebhart *et al.* [1] and the authors' is given in Table 2, where the values denoted by subscript G show

Table 1. Characteristic values of solution, accuracy and calculation

Pr	$f'(0)$	$h(0)/\sqrt{Pr}$	$2f(\infty)$	$\delta\sqrt{Pr}$	I	$(I_f - I_h)/I_h \times 10^5$	$\Delta\xi$	ξ_∞	$f'(\infty) \times 10^5$
0·01	0·5276	0·7214	19·28	3·341	1·00009	78	0·024	110·4	30
0·03	0·61745	0·64257	12·80	2·9923	1·00000	310	0·024	110·4	140
0·1	0·71033	0·56415	7·888	2·6471	1·00002	9·2	0·020	82·0	5·2
0·3	0·77544	0·49539	5·309	2·3714	1·00000	2·1	0·012	50·4	1·4
5/9	0·80093	0·45901	4·385	2·2413	1·00000	1·5	0·010	33·0	1·1
	[0·80093]	[0·45901]	[4·3844]	[2·24123]	[1]	[0]		[∞]	[0]
0·7	0·80872	0·44616	4·118	2·1982	1·00001	1·0	0·010	29·0	0·74
1	0·81937	0·42753	3·784	2·1385	0·99999	6·2	0·008	20·0	4·6
2	0·837485	0·396760	3·3418	2·0448	1·00000	0·63	0·007	25·9	0·46
	[0·837484]	[0·396761]	[3·3416]	[2·04477]	[1]	[0]		[∞]	[0]
3	0·84747	0·38240	3·179	2·0023	1·00001	1·2	0·006	25·6	0·88
5	0·85968	0·36786	3·039	1·9593	1·00000	5·7	0·005	23·0	4·2
10	0·87516	0·35336	2·918	1·9152	1·00000	1·6	0·004	25·4	1·1
30	0·98547	0·33889	2·818	1·8691	0·99999	6·7	0·003	24·6	4·7
100	0·91095	0·33018	2·766	1·8395	1·00001	4·9	0·002	26·6	3·4
∞	0·93356	0·31983	2·692	1·8024	1	—	—	—	—

The values of I correspond to the solutions obtained by using the values of $f'(0)$ and $h(0)$ in the second and third columns; $(I_f - I_h)/I_h$ is an index of accuracy for momentum conservation law, where $I_f = \int_0^\infty f'^2\,d\xi$ and $I_h = \frac{5}{4}\int_0^\infty h\,d\xi$; $\Delta\xi$ is division of ξ used in calculation; ξ_∞ is the largest value of ξ adopted in calculation; $f'(\infty)$ is the value of f' *at* ξ_∞; values in parenthesis [ ] correspond to the closed form solution; values for $Pr = \infty$ are quoted from [13].

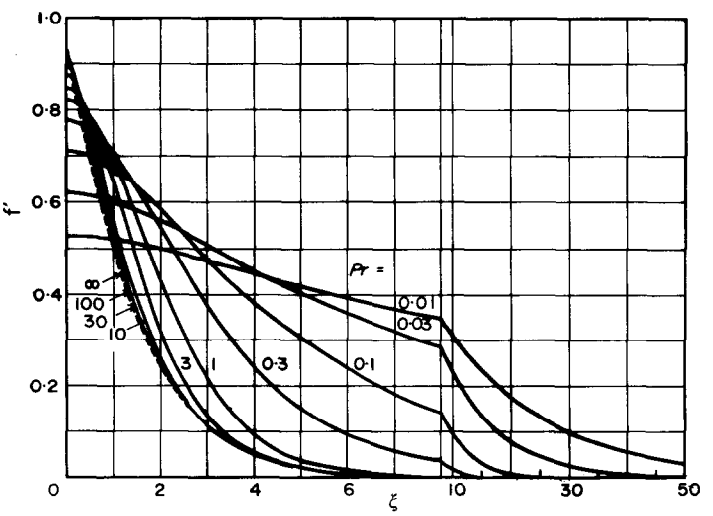

FIG. 1. Dimensionless profiles of vertical velocity component.

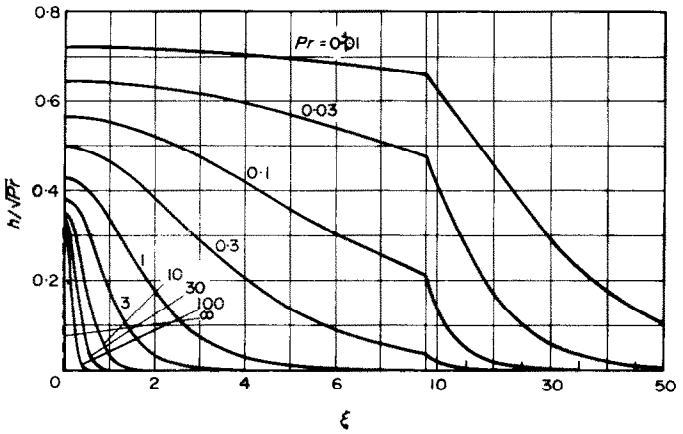

FIG. 2. Dimensionless profiles of temperature.

the results of Gebhart *et al.* converted into the authors' variables. The conversion is made by the following formulae,

$$\left.\begin{aligned} \xi_G &= (4^2J)^{\frac{1}{4}}\eta, \quad f_G = 4(4^2J)^{-\frac{1}{4}}F, \\ f'_G &= 4(4^2J)^{-\frac{1}{2}}F', \quad h_G = (4^3J^4)^{-\frac{1}{4}}H, \end{aligned}\right\} \tag{20}$$

where

$$J = \int_{-\infty}^{\infty} F'H\,\mathrm{d}\eta, \tag{21}$$

and η, F and H denote the variables of Gebhart *et al.* corresponding to ξ, f and h respectively.

The accuracy of solutions of Gebhart *et al.* is deteriorated with the increase of Pr number, namely with the increase of the thickness of velocity layer, as shown in Table 2. The range of employed for calculation affects eigenvalues $f''(0)$ and $h(0)$, and affects more remarkably the profiles and the values of $f(\infty)$, δ and I, which are shown in Table 1.

Figures 3 and 4 are prepared in order to interpolate the profiles for arbitrary Pr number. The values of $f''(0)$, $h(0)$ and δ in these figures are obtainable from Table 1 by interpolation.

Table 2. Comparison between the results of Gebhart et al. [1] *and the authors*

Pr	0·1	0·7	1	2	6·7	10
$f''_G(0)$	0·7065	0·8000	0·8098	0·8249	0·8469	0·8530
$f''(0)$	0·71033	0·80872	0·81937	0·83748	(0·8662)	0·87516
$\{f''_G(0) - f''(0)\} \times 100/f''(0)$	−0·5	−1·1	−1·2	−1·5	(−2·2)	−2·5
$h_G(0)$	0·1765	0·3653	0·4177	0·5444	0·8935	1·0619
$h(0)$	0·17840	0·37328	0·42753	0·56110	(0·9362)	1·11742
$\{h_G(0) - h(0)\} \times 100/h(0)$	−1·1	−2·1	−2·3	−3·0	(−4·5)	−5·0
$2f_G(\infty)$	7·913	4·169	3·831	3·384	3·008	2·940
$2f(\infty)$	7·888	4·118	3·784	3·342	(2·987)	2·918
$\{f_G(\infty) - f(\infty)\} \times 100/f(\infty)$	0·3	1·2	1·2	1·3	(0·7)	0·8
$f''_G/f''_G(0) = 0{\cdot}01$ at $\xi_G =$	20	7·5	6·6	6·1	6·0	6·0
$f''/f''(0) = 0{\cdot}01$ at $\xi =$	21·1	7·44	6·59	5·97	(5·93)	5·96
				[5·971]		
$h_G/h_G(0) = 0{\cdot}01$ at $\xi_G =$	24	7·1	5·6	3·6	1·8	1·4
$h/h(0) = 0{\cdot}01$ at $\xi =$	24·0	7·06	5·61	3·63	(1·73)	1·39
				[3·629]		

Values denoted by subscript G correspond to the results of Gebhart *et al.* [1] converted by (20) and (21); values in parenthesis ( ) are those interpolated from Table 1; values in brackets [ ] are those reckonend from the closed form solution.

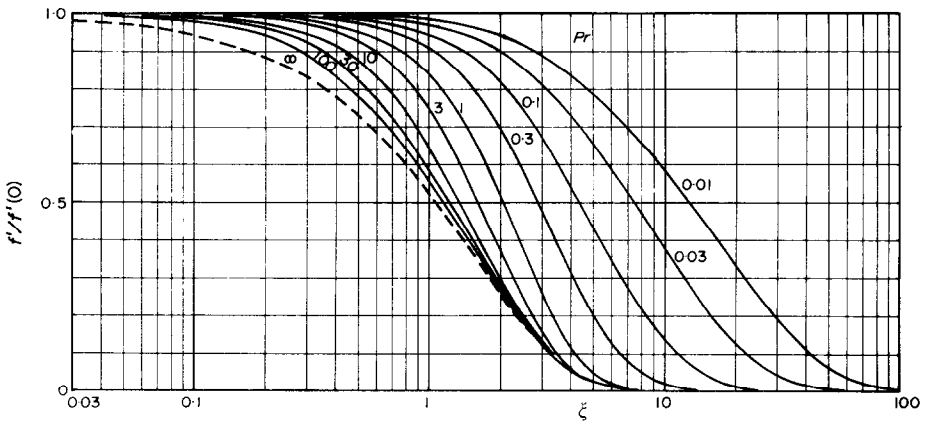

FIG. 3. Graph for interpolation of the profile of vertical velocity component for arbitrary *Pr* number.

4. EXPERIMENTAL RESULTS AND CONSIDERATIONS

4.1 *Apparatus*

The experiment for the plume in air was performed in a usual laboratory room, which was about $4 \times 5\,m^2$ in horizontal dimensions and about 4 m in height. A nichrome wire of 0·2 mm dia. was streached horizontally in 156 mm span between two copper blocks and placed about one meter from the bottom in the center of the room. The wire was heated by a direct electric current passing through it. The framework, which supported the wire, provided adjustments for horizontal leveling and for tensing the wire to preclude sag.

A 20 cm Mach–Zehnder interferometer was used to measure the temperature profile in the plume. The light source used was an electric spark with an interference filter passing 4480 Å light. Photographs of the interferogram were taken at a moment, when the image was relatively stationary, vertical and symmetrical. The fringe shift was converted to temperature variation by referring [16].

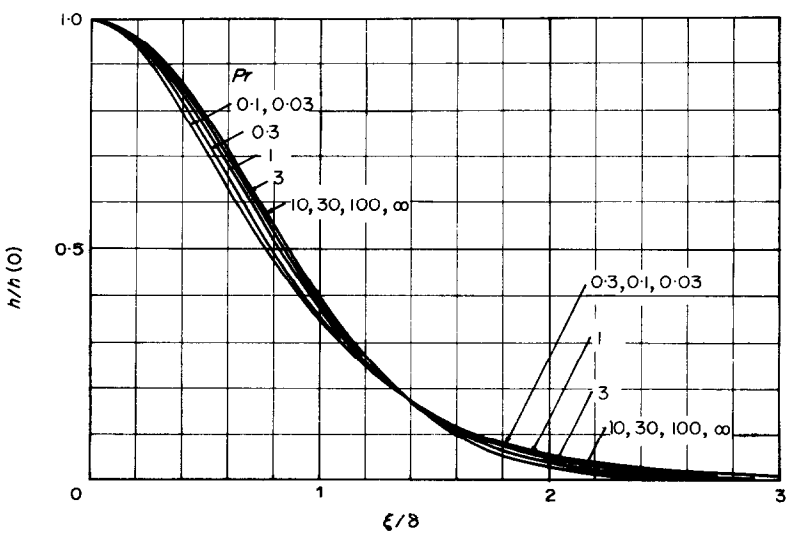

FIG. 4. Graph for interpolation of the profile of temperature for arbitrary *Pr* number.

The convection heat rate as the driving force of the plume was obtained by subtracting the radiant transfer rate from the electric input supplied to the wire. These heat rates were separated by calculation under the assumptions that the heat-transfer coefficient by natural convection is given by the expression of Senftleben [17] and that the emissivity of the surface of nichrome wire is equal to 0·7.

The experiments for the plumes in liquids were performed in tall and short acryle vessels, which were about 0·3 × 0·3 m^2 and 0·2 × 0·3 m^2 in horizontal dimensions and about 1·2 m and 0·3 m in height respectively. A sheath heater of 212 mm effective length and 1·0 mm outer dia. was used as the heat source. Two small flanges were attached to the sheath heater at places near the connecting points of resistance wire with lead wires, as shown in Fig. 5.

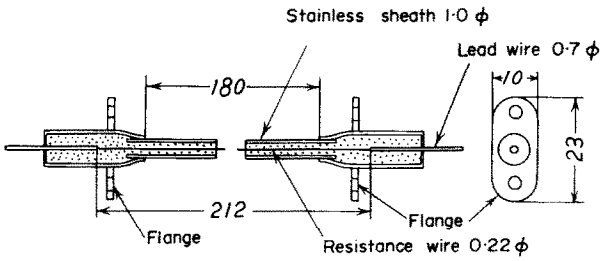

FIG. 5. Cross-section of the heat source used for the plumes in water and spindle oil.

In the tall vessel, the heater was supported just outside the flanges, and submerged about 0·1 m from the bottom. The levels of water and spindle oil were taken as 1·1 and 0·5 m. In the short vessel, the heater was attached between two parallel acryle plates at flanges, and submerged about 0·05 m from the bottom. In this vessel only water was used and the water level was about 0·25 m.

The temperature in the plume was measured by a copper–constantan thermocouple of 50 μm dia., which was stretched horizontally in 40 mm span and in vertical plane including the heat source. The thermo electro-motive force corresponding to the temperature rise above the ambient fluid temperature was recorded by a pen-recorder of 0·5 mV full-scale. The peak values on the recorder chart, on which the recorded curve was quasi-periodic, was evaluated as the maximum value at the elevation above the heat source.

Fluids used, dimensions of test space and heat source, and ranges of measurements, etc., together with those hitherto reported, are summarized in Table 3.

4.2 *Qualitative observation*

For the plume in air, the same characteristics as those found by Brodowicz–Kierkus [5] and Forstrom–Sparrow [6] were observed. Waves

Table 3. Apparatus and experimental conditions

		The authors			Brodowicz–Kierkus [3]	Forstrom–Sparrow [6]	Schorr–Gebhart [7]
Fluid		air	water	spindle oil	air	air	silicone
Pr		0·71	5·5–8	130–143	0·71	0·71	6·7
Space	m^3	4 × 5 × 4	0·2 × 0·3 × 0·25 and 0·3 × 0·3 × 1·1		1 × 1 × 2·5	0·8 × 0·6 × 1·1	0·14 × 0·19 × 0·25
Heat source							
dia.	mm	0·2	1·0	1·0	0·075	1·02	0·127
length	mm	156	212	212	250	254	51 & 153
Instrument		interferometer	thermocouple	thermocouple	interferometer	thermocouple	interferometer
Heat rate	W/m	24	60–220	60–410	9·75	2–13	1·56–2·8
Elevation	mm	8–16	10–20	20–200	10–80	6–380	7·6–78
Gr		1×10^5–1×10^6	1×10^5–2×10^6	3×10^3–2×10^7	7×10^4–4×10^7	4×10^3–5×10^9	3×10^4–7×10^7

In this Table are shown the ranges of the values employed for the discussion in the present paper.

of several Hz, which resembled those shown by Pera–Gebhart [8], took place occasionally. This phenomenon seemed to be a kind of selective resonance with natural turbulence in the ambient.

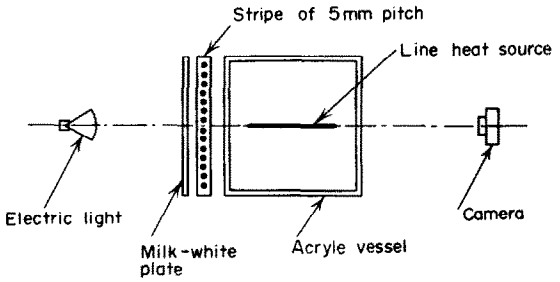

FIG. 6. Arrangement for photographing the plume in spindle oil.

The motion of the plumes in water and spindle oil was observed by utilizing the reflexion of light beam caused by the temperature variation under the situation shown in Fig. 6. Figure 7 shows the motion of the plume in spindle oil taken at about 20 s interval. Several lines rising from the heat source exhibit meandering of the plume along the direction of the center line of heat source. The plume usually swayed with meandering, and the whole form resembled closely to the fluttering of a flag, though the period of swaying was very slow, for example, about 5–10 min. Similar motion was also found in the case of the plumes in spindle oil above heat sources of 27 and 48 cm dia. by Miyabe–Katsuhara [18].

When the temperature of vessel wall was asymmetrical or when a circulation of the fluid took place in the vessel, the plume inclined and did not sway. The influence of liquid level on the motion of plume was not remarkable. In the case of relatively small heat rate, the characteristic motion showed decline, though only the part near the heat source was observed.

Such necking in of the plume as pointed out by Schorr–Gebhart [7] was not visible, because the plume was attached to side plates in the short vessel, and relatively tight flow rose up from the flanges in the tall vessel.

4.3 *Temperature profile in the plume*

Dividing (6) and (7) by $h(0)$ and δ respectively, we obtain

$$h/h(0) = Gr^{\frac{1}{4}}t/h(0), \tag{22}$$

$$\xi/\delta = Gr^{\frac{1}{4}}y/\delta x. \tag{23}$$

By substituting measured values of x, y, t and Q into the right-hand terms of above expressions, the temperature and the coordinates are reduced to be dimensionless and the comparison with the theoretical prediction expressed in Fig. 4 becomes available.

In Figs. 8(a) and (b) are summarized the data on air and liquid silicone respectively. For reckoning dimensionless values, physical properties are taken at the ambient temperature. Even if these are taken at the maximum temperature, the results are affected only slightly.

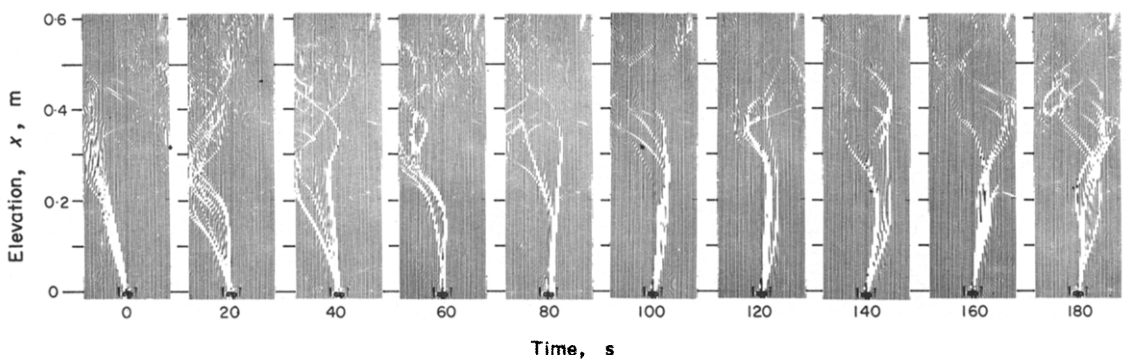

FIG. 7. Motion of a plume in spindle oil. Q = 404 W/m, time interval = 20 s.

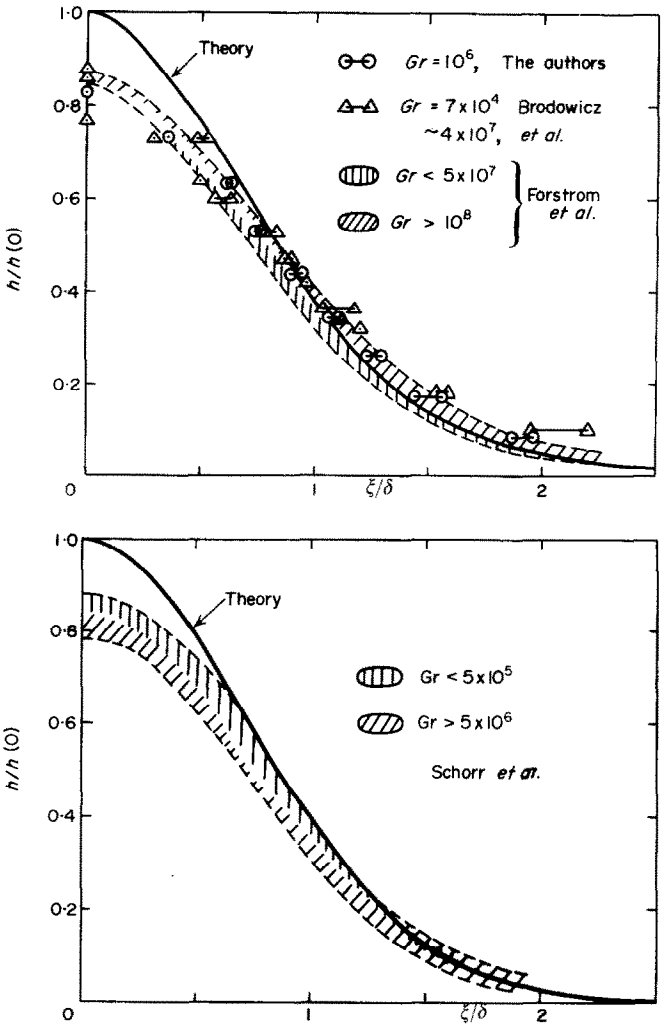

FIG. 8. Comparison between theory and experiment on the dimensionless profile of temperature. (a) air. $Pr = 0{\cdot}71$, $h(0) = 0{\cdot}375$, $\delta = 2{\cdot}605$ (b) silicone, $Pr = 6{\cdot}7$, $h(0) = 0{\cdot}932$, $\delta = 0{\cdot}745$.

Elevation x is measured from the center of heat source.

In Fig. 8(a) the data of Brodowicz–Kierkus are taken from Fig. 9 of [5]. For the data of the authors and Brodowicz–Kierkus, the connecting horizontal bars indicate the order of the uncertainty caused by the asymmetry of interferogram. Bands of scattering of the data of Forstrom–Sparrow are shown by broken lines. These are the data on laminar plume in Figs. 3 and 4 of [6], which are rearranged by the use of the values shown in Table 1 of [6]. Though slight influence of x is recognized on the scattering of data, most of the data in the ranges of $Gr < 5 \times 10^7$ and $Gr > 10^8$ are in the bands hatched vertically and obliquely respectively. This tendency is, in fact, corresponding to the idea of a virtual heat source. Though the data of authors and Brodowicz–Kierkus are in the range of lower Grashof number, they have relatively higher values of $h/h(0)$.

The broken lines in Fig. 8(b) show the bands

of data of Schorr–Gebhart, which are taken from Figs. 8, 9, 11 and 12 of [7] and rearranged by the use of the values Δt_0 shown in Figs. 5 and 6 of [7]. The data for $Q = 0{\cdot}7$ W/m of [7] are not adopted, because their values of $h/h(0)$ are too small. Though the data on 2 in. length heater are generally located near the upper line and those of 6 in. length heater near the lower line, there are also recognized the tendency that the larger Grashof number the lower value of $h/h(0)$ and the smaller Grashof number the higher value, whether the heat source is longer or shorter, as shown in Fig. 8(b). This tendency is inconsistent with the results of Forstrom–Sparrow and constitutes a ground opposed to the idea of a virtual source.

Despite that the data summarized in Fig. 8(a) were obtained under different conditions, as shown in Table 3, and under very different circumstances as mentioned previously, the general tendency is the same with each other; that is, the maximum temperature measured is about 15–20 per cent lower and the outer part of the plume is more extensive in comparison with theoretical predictions. The scattering of the data is also in similar order for all experiments, and it is smaller than the difference between theory and experiment. Therefore, it is reasonable at present that the origin of x is taken at the center line of the heat source.

It may be considered that both the difference between theory and experiment and the scattering of data are affected by the mode of swaying and meandering. Though the profile measured is different from the theoretical prediction, the similarity, i.e. the functional relation among x, y, t and Q is admittedly consistent.

By the way, Forstrom–Sparrow and Schor–Gebhart took the maximum of measured values as the representative for dimensionless expressions, stating that the measured values were in excellent agreement with theory. This comparison is unreasonable, and at the same time the accuracy of the profile depends on that of the maximum value.

4.4 *Maximum temperature in the plume*

From (6) the following expression is obtained,

$$t_0/\Theta h(0) = Gr^{-\frac{1}{4}}, \tag{24}$$

where t_0 is the temperature at the mid-plane of the plume. The relation of $t_0\Theta h(0)$ vs. Gr is plotted in Fig. 9, where t_0 is the mean value of maximum temperature measured at x, $h(0)$ is interpolated from Table 1, Θ and Gr are reckoned from respective experimental conditions, and physical properties of water and spindle oil at the ambient temperature are evaluated by the use of the formulae in Appendix of [19]. The references of the data hitherto reported are made similarly as in previous section.

For water and spindle oil, the data in the range

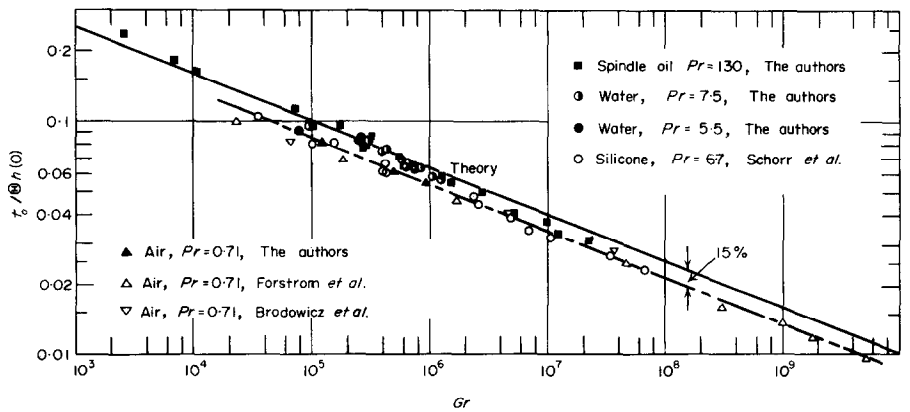

FIG. 9. Comparison between theory and experiment on the relation of $t_0/\Theta h(0)$ vs. Gr.

of about $Gr < 10^6$ are in good agreement with theory, whereas those in the range of about $Gr > 10^6$ are about 10–15 per cent lower than the theoretical prediction. The influence of the liquid level on these data was not appreciable.

All data for air are about 15–20 per cent lower than theoretical predictions. The swaying and meandering of the plume may be appreciated from local point of view as fluctuations of temperature and velocity. It may be possible to raise the homogenizing of the fluctuations in the plume in air, since the periods of swaying and meandering of the plume in air are relatively small and the temperature diffusivity of air is relatively large. It is, however, not able to explain why the results for liquid silicone by Schorr–Gebhart [7] show tendencies different from those for water in the ranges of smaller Gr number, though the physical properties of the both are in the same order.

5. CONCLUSION

(1) The closed form solution of pertinent equations is obtainable only for the cases of $Pr = \frac{5}{9}$ and 2.

(2) The idea of boundary conditions by Gebhart *et al.* [1] does not lead to any new conceptions.

(3) New accurate numerical solutions are obtained for $Pr = 0{\cdot}01$, $0{\cdot}03$, $0{\cdot}1$, $0{\cdot}3$, $0{\cdot}7$, 1, 3, 5, 10, 30 and 100. The characteristic values are shown in Table 1, and the graphs for interpolation of the profiles of vertical velocity component and temperature for arbitrary Pr number are given in Figs. 3 and 4 respectively.

(4) Gebhart *et al.* contributed only a little on numerical calculation, and there are errors of the order of several per cent in their results.

(5) The plume usually sways and meanders with the similar mode as the fluttering of a flag. An example of the motion of the plume in spindle oil is shown in Fig. 7. The similar instability as shown by Pera–Gebhart [8] was also observed occasionally in the experiment for air.

(6) When the plume comes right above the heat source, the maximum temperature is in good agreement with theoretical prediction in the range of about $Gr < 10^6$ for the plumes in water and spindle oil. All data for the maximum temperature in the plume in air are about 15–20 per cent lower than theoretical prediction.

(7) The temperature distributions for the plumes in air and liquid silicone are different from theory, but the similarity relation is consistent with theory.

(8) It would be better to consider that the difference between theory and experiment and the scattering of data is due more to the variation of the mode of meandering and swaying than to the accuracy of the measurement and/or the carefulness on experimental procedure.

ACKNOWLEDGEMENTS

The authors acknowledge the cooperation of graduate student T. Tsuji in the experiment. Messrs T. Abe, M. Kinoshita, S. Nagaoka and K. Hanada took part in this study as part of their graduation thesis. Numerical computations were performed with an electronic computer FACOM 230-60 in Computer Center, Kyushu University.

REFERENCES

1. B. GEBHART, L. PERA and A. W. SCHORR, Steady laminar natural convection plumes above a horizontal line heat source, *Int. J. Heat Mass Transfer* **13**, 161–171 (1970).
2. A. M. SOWARD, Steady free convection above a point heat source and a horizontal line heat source in a vertical magnetic field, *J. Fluid Mech.* **39**, 753–780 (1969).
3. K. BRODOWICZ, Diffuse free convection in a jet above an axially symmetric orifice during hydrogen outflow into ambient air, *Int. J. Heat Mass Transfer* **13**, 1243–1248 (1970).
4. S. B. SAVAGE and G. K. C. CHAN, The buoyant two-dimensional laminar vertical jet, *Q. J. Mech. Appl. Math.* **23**, 413–430 (1970).
5. K. BRODOWICZ and W. T. KIERKUS, Experimental investigation of laminar free-convection flow in air above horizontal wire with constant heat flux, *Int. J. Heat Mass Transfer* **9**, 81–94 (1966).
6. R. J. FORSTROM and E. M. SPARROW, Experiments on the buoyant plume above a heated horizontal wire, *Int. J. Heat Mass Transfer* **10**, 321–331 (1967).
7. A. W. SCHORR and G. GEBHART, An experimental investigation of natural convection wakes above a line heat source, *Int. J. Heat Mass Transfer* **13**, 557–571 (1970).

8. L. PERA AND B. GEBHART, On the stability of laminar plumes; some numerical solutions and experiments, *Int. J. Heat Mass Transfer* **14**, 975–984 (1971).
9. T. FUJII, Theory of the steady laminar natural convection above a horizontal line heat source and a point heat source. *Int. J. Heat Mass Transfer* **6**, 597–606 (1963).
10. CHIA-SHUN YIH, Free convection due to a line source of heat, *Trans. Am. Geophys. Un.* **33**, 669–672 (1962).
11. L. J. CRANE, Thermal convection from a horizontal wire, *Z. Angew. Math. Phys.* **10**, 453–460 (1959).
12. R. S. BRAND and F. L. LAHEY, The heated laminar vertical jet, *J. Fluid Mech.* **29**, 305–315 (1967).
13. D. B. SPALDING and R. G. CRUDDACE, Theory of the steady laminar buoyant flow above a line heat source in a fluid of large Prandtl number and temperature-dependent viscosity, *Int. J. Heat Mass Transfer* **3**, 55–59 (1961).
14. Y. KATTO and T. KOIDE, A note on vectorial dimensional analysis and similarity solutions (in Japanese), NAL TM-9, 1–12 (1963).
15. H. UEHARA and T. FUJII, Natural convection above a horizontal line heat source and a point heat source (the continued report)—Numerical solution for the steady laminar flow—(in Japanese), Report of Research Institute of Industrial Science of Kyushu University, No. 38, 1–87 (1964).
16. R. W. LADENBURG, *Physical Measurements in Gas Dynamics and Combustion*, p. 47. Princeton Univ. Press, New Jersey (1954).
17. H. SENFTLEBEN, Die Wärmeabgabe von Körpern verschiedener Form in Flüssigkeiten und Gasen bei freier Strömung, *Z. Angew. Phys.* **3**, 361–373 (1951).
18. K. MIYABE and T. KATSUHARA, Experimental investigation on the swaying plume above heated horizontal cylinders, *Mem. Kyushu Inst. Technol.* No. 2, 9–22 (1972).
19. T. FUJII, M. TAKEUCHI, M. FUJII, K. SUZAKI and H. UEHARA, Experiments on natural-convection heat transfer from the outer surface of a vertical cylinder to liquids, *Int. J. Heat Mass Transfer* **13**, 753–787 (1970).

SILLAGE NATUREL AU-DESSUS D'UNE SOURCE THERMIQUE LINEAIRE HORIZONTALE

Résumé—Le premier problème traité dans cet article est la résolution des équations concernant le sillage laminaire permanent au-dessus d'une source thermique linéaire horizontale. Tandis que la solution de Gebhart *et al* proposée pour ce problème est la cause de controverses, de nouvelles solutions numériques plus précises sont présentées pour $Pr = 0{,}01$, 0,03, 0,1, 0,3, 0,7, 1, 3, 5, 10, 30 et 100. De plus, les profils de la composante verticale de la vitesse et les profils de température ont été donnés graphiquement afin de permettre une interpolation pour un nombre de Prandtl arbitraire.

Puis on a considéré la relation entre la théorie et l'expérience a travers la révision des résultats des expériences déjà faites sur les illages dans l'air, l'eau et l'huile aussi bien que ceux jusqu'ici rapportés sur l'air et le silicone liquide. Le mouvement naturel du sillage non perturbé est très lent et fait penser au au flottement d'un drapeau. Les photographies présentées ici représentent le mouvement typique du panache dans l'huile. De façon générale, les résultats expérimentaux sont différents de ceux théoriques mais, lorsque l'on considère la distribution de température dans le panache, on peut lui appliquer la variable de similarité correspondant à la théorie. Les températures maximales des sillages dans l'air sont d'environ 15 à 20 pour cent inférieures aux estimations théoriques dans le domaine complet du nombre de Grashof. Celles enregistrées dans l'eau et l'huile sont en bon accord avec les estimations théoriques dans le domaine de $Gr < 10^6$.

AUFTRIEBSSCHLIEREN ÜBER EINER HORIZONTALEN, LINIENFÖRMIGEN WÄRMEQUELLE

Zusammenfassung—Das erste Problem, das in dieser Arbeit behandelt wird, ist die Lösung der Gleichungen für die Bewegung der stationären laminaren Schlieren über einer horizontalen, linienförmigen Wärmequelle. Da einige Widersprüche zu den Aussagen von Gebhart et. al. [1] zu diesem Thema erhoben wurden, sind genauere numerische Lösungen für $Pr = 0{,}01$; 0,03; 0,1; 0,3; 0,7; 1; 3; 5; 10; 30 und 100 angegeben. Außerdem werden die Profile der vertikalen Geschwindigkeitskomponente und der Temperatur so aufgezeichnet, dass sie sich zur Interpolation für beliebige Prandtl-Zahlen eignen.

Dann wird die Beziehung zwischen Theorie und Experiment untersucht, unter Berücksichtigung aller experimentellen Ergebnisse über Auftriebsschlieren in Luft, Wasser und Spindelöl ebenso wie der bisher veröffentlichten Ergebnisse für Luft und flüssiges Silikon. Da die natürliche Bewegung einer ungestörten Schliere extrem langsam ist, hat sie beträchtliche Ähnlichkeit mit dem Flattern einer Flagge. Die hier gezeigten Fotos stellen die typische Bewegung einer Auftriebsschliere in Spindelöl dar.

Allgemein unterscheiden sich die Versuchsergebnisse von der Theorie für die Temperaturverteilung in der Schliere, doch lässt sich die Ähnlichkeitsvariable aus der Theorie auf das Experiment anwenden. Die Maximaltemperaturen der Schlieren in Luft liegen im ganzen Bereich der Grashof-Zahl etwa 15 bis 20% tiefer als die theoretischen Voraussagen. In Wasser und im Spindelöl stimmen sie im Bereich $Gr < 10^6$ gut mit der Theorie überein.

КОЛЕБЛЮЩИЙСЯ ОРЕОЛ НАД ГОРИЗОНТАЛЬНЫМ ЛИНЕЙНЫМ ИСТОЧНИКОМ ТЕПЛА

Аннотация—Первой задачей, рассматриваемой в данной статье, является решение уравнений для стационарного ламинарного ореола над горизонтальным линейным источником тепла. Несмотря на некоторые расхождения со взглядами Гебхарта и др. 1 по этой задаче, получены более точные численные решения для $Pr = 0{,}01$; 0,03 ; 0,1 ; 0,3 ; 0,7 ; 1, 3,5, 10,30 и 100. Кроме того, профили вертикальной компоненты скорости и температуры представлены так, что эти результаты могут быть использованы при интерполировании для произвольного значения числа Прандтля.

Приводится сопоставление теоретических и экспериментальных данных, для чего выполнен обзор экспериментальных результатов по ореолам в воздухе, воде и веретенном масле, а также ранее сообщенных данных по воздуху и жидкому силикону. Естественное движение невозмущенного ореола спокойное, очень медленное и напоминает трепетание флага. На представленных фотографиях показано характерное движение ореола в веретенном масле. Вообще говоря, экспериментальные результаты отличаются от теоретических, но поскольку рассматривается распределенте температуры в ореоле, то к нему может быть применена соответствующая теории автомодельная переменная. Максимальные температуры в ореолах в воздухе оказались примерно на 15–20% ниже, чем в теоретических расчётах для всего диапазона значений числа Грасгофа. Что касается воды и веретенного масла, то здесь наблюдалось хорошее соответствие с теоретическими данными в диапазоне $Gr < 10^6$.